

## INVESTIGATIONS OF THE ROTATION POLE FROM THE MORPHOLOGY OF DUST FANS OF COMET 81P/WILD 2

R. VASUNDHARA

Indian Institute of Astrophysics, Koramangala, II Block, Bangalore 560034, India; rvas@iiap.res.in

AND

PAVAN CHAKRABORTY

Inter-University Centre for Astronomy and Astrophysics, Post Bag Number 4, Ganeshkhind,  
Pune 411007; and Assam University, Silchar 788011, India; pavan@iucaa.ernet.in

Received 2003 October 22; accepted 2004 July 12

### ABSTRACT

Investigations of the dust morphology of comet 81P/Wild 2 in the *I*- and *R*-band images obtained on 1997 May 15 from the Vainu Bappu Observatory, Kavalur, India, are presented. We model the trajectories of dust grains ejected from distributed sources on this comet to explain the morphology of the fans in these images and in the published images by Schulz and coworkers. We derive the pole position of  $\alpha_p = 297^\circ \pm 5^\circ$  and  $\delta_p = -10^\circ \pm 5^\circ$ . Broad sources at  $+80^\circ \pm 5^\circ$  and  $-25^\circ \pm 5^\circ$  latitudes best explain the northern and southern fans, respectively.

*Subject headings:* comets: general — comets: individual (81P/Wild 2) — space vehicles

### 1. INTRODUCTION

Comet 81P/Wild 2 was visited by NASA's *Stardust* mission on 2004 January 2. A member of the Jupiter family since its encounter with Jupiter in 1974, this comet has had only four perihelion passages closer to  $\approx 1.5$  AU. Fink et al. (1999) find the comet to be dusty. Evidence of fans arising as a result of distributed sources and the possibility of the spacecraft intercepting one of the dust streams have been pointed out by Schulz et al. (2003) and Farnham & Schleicher (2002). Sekanina (2003) used the position angles of the fan structures from this comet in the images of Schulz et al. (2003) obtained on 1996 December 11 and 1997 April 2 to derive the direction of its rotation axis as  $\alpha_p = 297^\circ$  and  $\delta_p = -5^\circ$ . Farnham (2003) used the position angle of the primary fan in the seven images between 1997 February 1 and 1997 October 1 to derive the pole position  $\alpha_p = 281^\circ$  and  $\delta_p = +13^\circ$  (T. L. Farnham 2003, private communication, correcting the numbers in the abstract). Using additional moderately large field imaging data taken on 1997 April 1, provided by M. J. I. Brown & R. L. Webster (2003, private communication), and images of this comet from the Vainu Bappu Observatory, Kavalur, India, taken on 1997 May 15, we carry out simulations of the trajectories of dust grains in the fans to match the initial direction and curvature of the fans to further constrain the rotation axis.

### 2. OBSERVATIONS AND DATA PROCESSING

The observations (filter imaging) of comet Wild 2 were carried out at the prime focus ( $f/3.3$ ) of the 2.34 m telescope at the Vainu Bappu Observatory on 1997 May 15. A TK1024 photometric liquid-nitrogen-cooled CCD yielded a field of  $11' \times 11'$  with a resolution of  $0''.6$  pixel $^{-1}$ . The seeing at the time of observation was  $\sim 2''$ . Images were obtained through Cousins *R* and *I* filters. Table 1 gives the log of these selected observations. The images after bias subtraction, flat-fielding, and sky subtraction were stacked to form combined *R*- and *I*-filter images after carefully aligning them. The aligning of the images was attempted at subpixel accuracies by determining the comet center in each of the images using the task *imcentroid* of the IRAF package at the location of the brightest pixel. A

centering box of 3 pixel was selected for this task. The task *imshift* of the same package was used to shift the centroid to the middle of the pixel for each image before trimming and stacking. The faint features embedded in the coma were delineated by dividing the image by a synthetic coma with a radial variation of  $r_c^{-1}$ .

The combined *R*- and *I*-filter images normalized by the synthetic coma appeared identical, indicating major contribution from the dust in the coma. Hence, to further improve the signal-to-noise ratio (S/N), the *R* and *I* sets of images were combined. The processed image in Figure 1 (*left*) shows three distinct features: (1) the most prominent structure along the antisunward direction corresponding to the dust tail; (2) an extended fan along the northeast from source I (Sekanina 2003); although merged with the antisunward tail, this feature is conspicuous because of its extension north of the tail axis; and (3) a fan along the southwest due to source II. The Gaussian convolved image on the right in Figure 1 with a  $\sigma$  of 1 pixel shows these features more clearly.

### 3. TRAJECTORIES OF THE DUST GRAINS IN THE JETS

An acceptable solution of the pole axis must adequately explain the fan/jet morphology at different epochs. We also make use of the published images of 1996 December 11 and 1997 April 2 by Schulz et al. (2003) and the image of 1997 April 1 by M. J. I. Brown & R. L. Webster (2003, private communication). Details of these observations are given in Table 1. The computer simulations were carried out using the model by Vasundhara (2002) explained briefly in the following section. This model adopts the basic concepts introduced by Sekanina (1981a, 1981b, 1991).

#### 3.1. The Model

The model predicts the loci of the dust grains as seen projected on the sky plane relative to the comet at any instant of time. The sources are assumed to emit jets of gas and dust from local sunrise to sunset. The ejected grains are subjected to the gravitational attraction of the Sun and the solar radiation pressure force in the opposite direction. Relative to the comet,

TABLE 1  
LOG OF OBSERVATIONS OF COMET WILD 2 AND VIEWING GEOMETRY

Date	UT	Telescope (m)	Filter	Image Scale (arcsec pixel <sup>-1</sup> )	$T_{\text{exp}}$ (s)	$r$ (AU)	$\Delta$ (AU)	$PA_{\odot}$ (deg)	Phase (deg)	$B$ (deg)	$B'$ (deg)	$P$ (deg)	Reference
1997 May 15.....	15:55	2.34	<i>I</i>	0.6	4 × 90	1.24	1.58	289.5	39.6	60.0	22.7	81.4	1
1997 May 15.....	16:11	2.34	<i>R</i>	0.6	5 × 90	1.24	1.58	289.5	39.6	60.0	22.7	81.4	1
1997 Apr 2.....	01:26	1.5	<i>R</i>	0.39	180	1.62	0.992	283.4	35.7	76.5	48.5	30.6	2
1997 Apr 1.....	09:26	1.02	<i>R</i>	1.2	40	1.62	0.989	283.5	35.5	76.7	48.9	29.8	3
1996 Dec 11.....	06:15	2.2	<i>R</i>	0.262	300	2.11	1.29	106.2	19.1	79.4	74.9	52.4	2

REFERENCES.—(1) This paper; (2) Schulz et al. 2003; (3) M. J. I. Brown & R. L. Webster 2003, private communication.

the position of the dust grains can be calculated from their initial velocity, the radiation pressure force, and the ejection geometry.

### 3.1.1. Velocity and Acceleration of the Grains

On leaving the nucleus radially, the dust grains move under the combined force of solar radiation pressure and solar gravity. We neglect the gravitational force of the nucleus. The thermal velocity of the gas  $v_g$  at heliocentric distance  $r$  was calculated using the relation by Delsemme (1982),

$$v_g = 0.58r^{-0.5}. \quad (1)$$

The initial grain velocity  $v(a)$  of a grain of radius  $a$  was computed using the expression by Sekanina (1981b),

$$v(a) = v_g \left[ \frac{1}{3} \left( 1 + \frac{0.65}{1 + \alpha_a^{2/3}} \right) (1 + 0.38\psi^{0.68}) + 0.225\alpha_a^{1/2} \right]^{-1}, \quad (2)$$

where the accommodation coefficient  $\alpha_a$  is defined by

$$\alpha_a = 3.13 \frac{v_g \rho a}{\mu_g R_N}.$$

The acceleration  $\alpha = (\beta g_{\text{sun}(1)})/r^2$  due to solar radiation pressure depends on the nature of the grain  $\beta$  and the helio-

centric distance  $r$ , where  $g_{\text{sun}(1)}$  is the acceleration due to solar gravity at 1 AU ( $0.6 \times 10^{-5} \text{ km s}^{-2}$ ). Using the definition of  $\beta$  (Finson & Probst 1968) as the ratio of the force due to solar radiation pressure,

$$\beta = F_{\text{rad}}/F_{\text{grav}} = \frac{3Q_{\text{pr}}E_{\odot}}{4\pi cGM_{\odot}} \frac{1}{\rho a}, \quad (3)$$

where  $Q_{\text{pr}}$  is the scattering efficiency for radiation pressure of the grain,  $\rho$  is its density,  $E_{\odot}$  is the total solar radiation  $\text{s}^{-1}$ ,  $c$  is the velocity of light,  $M_{\odot}$  is the mass of the Sun, and  $G$  is the universal gravitational constant. In the present investigation, the lower and upper limits on the grain size were taken as  $a_{\text{min}} = 0.05 \mu\text{m}$  and  $a_{\text{max}} = 30 \mu\text{m}$ , respectively.

### 3.1.2. Sky-Plane Coordinates of the Dust Grain Relative to Comet Center

In order to trace the trajectories of grains from distributed regions on the comet, we found it convenient to first compute the grain locations at different times in the cometocentric frame and then compute their projected sky-plane positions with respect to the projected comet center.

A dust grain ejected from an active region  $G(u, \phi, R, t = 0)$  at longitude  $u$  and latitude  $\phi$  on the surface of a spherical nucleus of radius  $R$  (Fig. 2) radially traverses a distance  $v_{\text{gr}}t$  outward from the comet and a distance  $(1/2)\alpha t^2$  along the Sun-comet direction due to solar radiation pressure during time  $t$ . At distances that are large compared to the size of the nucleus,

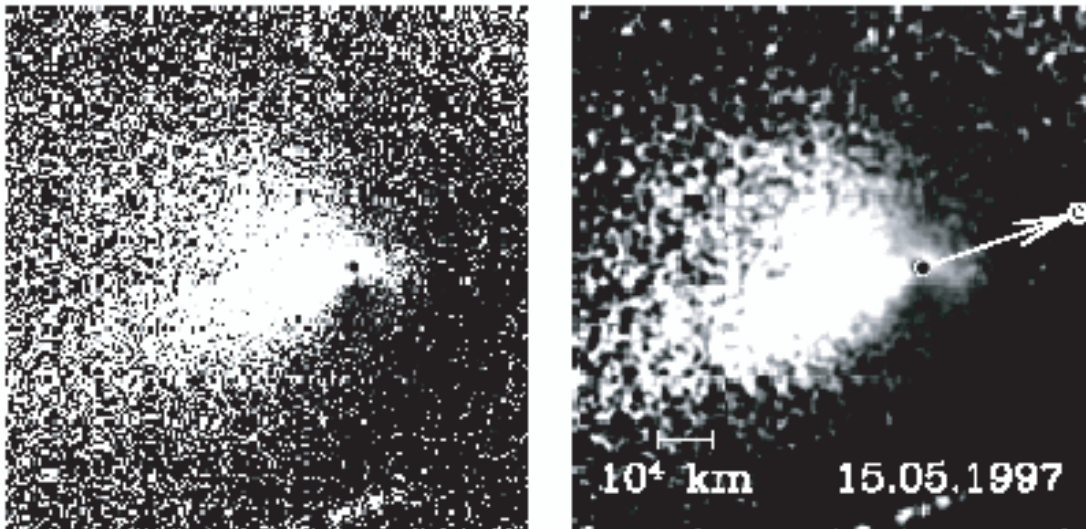


FIG. 1.—Left: Stacked, normalized, and combined *I* and *R* image of 1997 May 15 from the Vainu Bappu Observatory. East is to the left and north is to the top. Right: Gaussian-convolved image with a  $\sigma$  of 1 pixel to smooth the noise.

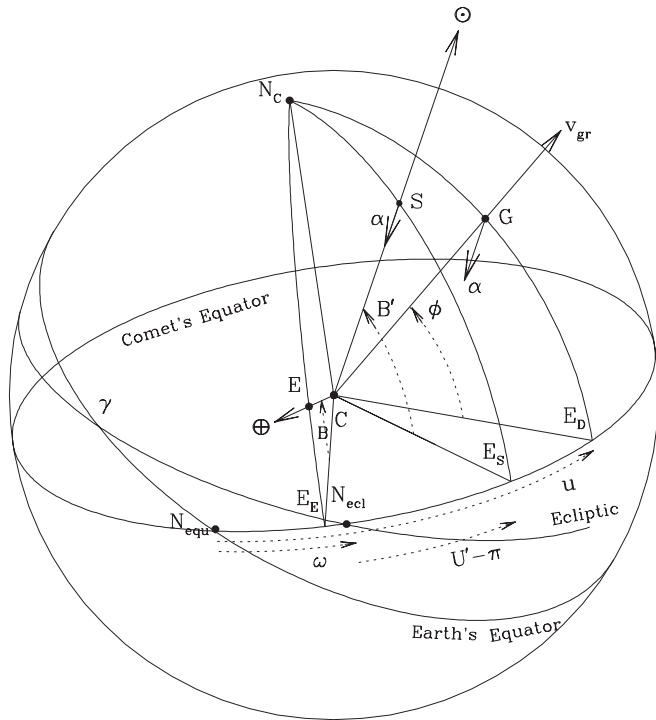


FIG. 2.—Adapted from Vasundhara & Chakraborty (1999), geometry indicating the sub-Earth point (E), sub-Sun point (S), active region (G) on the comet, and angles in eq. (4).

the longitude  $u'$ , latitude  $\phi'$ , and radial distance  $r'$  ( $u'$ ,  $\phi'$ ,  $r'$ ,  $t = t$ ) of the grain is given by

$$\begin{aligned} r' \cos \phi' \cos u' &= v_{gr} t \cos \phi \cos u - (1/2) \alpha t^2 \cos B' \cos U'' \\ r' \cos \phi' \sin u' &= v_{gr} t \cos \phi \sin u - (1/2) \alpha t^2 \cos B' \sin U'' \\ r' \sin \phi' &= v_{gr} t \sin \phi - (1/2) \alpha t^2 \sin B', \end{aligned} \quad (4)$$

where  $U''$  is the longitude of the sub-Sun point  $S$  measured from  $N_{equ}$  and  $B'$ , the cometocentric latitude of the Sun. From Figure 2,

$$U'' = \omega + U' - \pi,$$

where  $\omega$  is the distance of  $N_{ecl}$  from  $N_{equ}$  measured on the equator of the comet and  $U' - \pi$  is the cometocentric longitude of the Sun measured along the direction of rotation of the comet from  $N_{ecl}$ .

The cometocentric coordinates ( $u'$ ,  $\phi'$ ,  $r'$ ,  $t$ ) of the grains measured on the comet's equator were then transformed to the cometocentric spherical coordinates with respect to the Earth's equator ( $A$ ,  $D$ ,  $r'$ ,  $t$ ), where  $A$  and  $D$  are the cometocentric right ascension and declination of the grain. This transformation depends on the direction of the pole of the comet and was carried out using the equations by Rhode & Sinclair (1992). The geocentric spherical coordinates of the dust grain were calculated from ( $A$ ,  $D$ ,  $r'$ ) and the geocentric coordinates of the comet using the rigorous expressions involving the cometocentric Earth's equatorial coordinates of the sub-Earth point and the grain (Gurnette & Woolley 1961).

#### 4. AVAILABLE INPUTS FOR MODELING THE IMAGES

Details of the images used in the present investigation are given in Table 1. From a holistic analysis of the water production curve of the comet over a period of  $\pm 100$  days from perihelion and the fans observed before and after perihelion, Sekanina (2003) proposed a two-source model. The northern source at  $+82^\circ$  and the near-equatorial one at  $-25^\circ$  occupy 11% to nearly 30% of the total area of the nucleus. The images sent back by *Stardust*<sup>1</sup> imply large bright areas consisting of clusters of distributed sources. Following Hanner & Hayward (2003), the values of the grain density  $\rho$ , gas mass production

<sup>1</sup> Information about *Stardust* can be found at <http://stardust.jpl.nasa.gov>.

TABLE 2  
PARAMETERS USED IN THE MODEL

Parameter	Symbol	Value	Status	Reference
Radius .....	$R_N$	2.0 km	Adopted	1
Dust/gas mass ratio .....	$\psi$	0.4	Adopted	1
Gas mass flux.....	$\mu_g$	$7.6 \times 10^{-6} \text{ g cm}^{-2} \text{ s}^{-1}$	Adopted	1
Density of grains.....	$\rho$	$1 \text{ g cm}^{-3}$	Adopted	1
Size distribution law of Sekanina-Hanner with .....	$M$	8.14	Adopted	1
	$N$	1.7	Adopted	1
	$a_0$	0.05 $\mu\text{m}$	Adopted	1
Grain sizes .....	$a$	0.05–30 $\mu\text{m}$	Adopted	1
Grain refractive index.....	...	$1.7+i 0.1$	Adopted	1
Position of rotation axis.....	$\alpha_p$	$297^\circ$		2
(J2000) .....	$\delta_p$	$-5^\circ$		
Position of rotation axis.....	$\alpha_p$	$297^\circ \pm 5^\circ$	Derived	3
(J2000) .....	$\delta_p$	$-10^\circ \pm 5^\circ$		
Latitude of active regions .....				
Source I.....				
Latitude .....	$\phi I$	$+80^\circ \pm 5^\circ$	Derived	3
Latitude span.....		$+50^\circ$ to $+85^\circ$		
Relative activity .....		$\sim 50\%$ at $+80^\circ \pm 5^\circ$		
Source II.....				
Latitude .....	$\phi II$	$-25^\circ \pm 5^\circ$	Derived	3
Latitude span.....		$-40^\circ$ to $+10^\circ$		

REFERENCES.—(1) Hanner & Hayward 2003; (2) Sekanina 2003; (3) this paper.

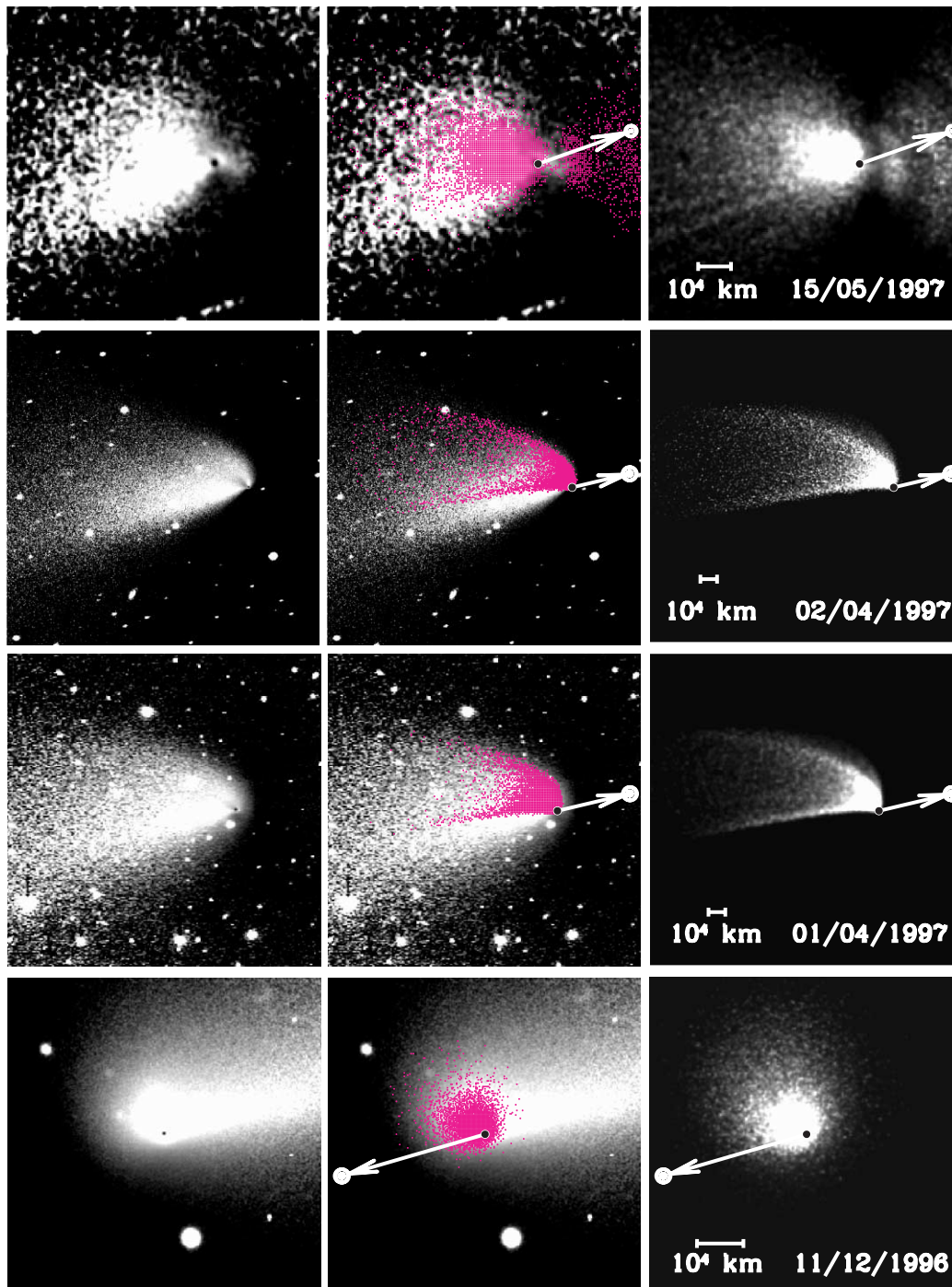


FIG. 3.—*Left*: Observed images normalized with synthetic coma. *Right*: Simulated images using a period of 0.5 day. *Middle*: Simulated fans superposed on the observed images.

flux  $\mu_q$ , and nuclear radius  $R_N$  used in the present study are given in Table 2. Of the two size distributions discussed by Hanner & Hayward (2003), we have selected the Sekanina-Hanner distribution; in the optical region, grains covered by this distribution are more relevant.

#### 5. EFFECT OF ROTATION PERIOD ON DUST MORPHOLOGY

In addition to the pole direction of the nucleus and the location of the active regions, the period of rotation of the nucleus influences the morphology of the fans. For a source continuously lit by the Sun during the day, short periods of

rotation at large heliocentric distances produce tightly wrapped shells resembling a cone. The edges will appear as pairs of jets, as in the 1997 October and 1997 November images of comet Hale-Bopp. On the other hand, long periods of rotation will produce asymmetric fans/arcs (Sekanina & Larson 1984), because of the large differences in the distances traveled by the grains ejected during one rotation of the nucleus. When the period of rotation of the nucleus is comparable to the time taken by a grain to traverse the distance spanning the CCD frame, a single feature will be expected. This feature will trace the cone of revolution of a short-period nucleus but with a large pitch angle for the same source. The absence of distinct shell

patterns in the 1997 April and May images of comet Wild 2 imply either that the rotation period is very small (a few hours), so that the shells overlapped, or that the source may be extended. On the other hand, if the period is very large (several days), the entire fan must have been created during a single rotation. Attempts to detect rotation from brightness variations near aphelion have not been successful (Meech & Newburn 1998; Farnham & Schleicher 2002). Hence, the rotation period of the nucleus of comet Wild 2 is still an unsettled issue. In the present investigation, following the short-period scenario, we take advantage of the fact that as long as the period is short and the shells are not resolved, knowledge of the actual period is not essential for carrying out the modeling; thus, we assume a period of 0.5 day for the computations.

## 6. FIT TO THE DATA

The simulations were carried out to include grains ejected during eight rotations. To understand the morphology of the dust features, assumptions of spherical grains and Mie scattering were considered adequate to compute the light-scattering functions and  $Q_{pr}$  in equation (3). As a first guess of the range of possible pole solutions, we looked at all values of  $(\alpha_p, \delta_p)$  in the ranges  $0^\circ \leq \alpha_p \leq 360^\circ$  and  $-90^\circ \leq \delta_p \leq +90^\circ$ . We selected a range of values of these parameters for which the position angles of the visible pole were within  $\pm 10^\circ$  of the observed position angles of Fan I (from source I) in the 1996 December 1 and 1997 April 1 and 2 and May 15 images. The possible solutions varied between  $\alpha_p = 280^\circ$ ,  $\delta_p = +15^\circ$  and  $\alpha_p = 300^\circ$ ,  $\delta_p = -15^\circ$ . These pole directions were used as initial parameters in the modeling. Large fields in the 1997 April 1 and 2 images helped to trace Fan I to distances of  $\sim 10^5$  km. Modeling of the curvature and cross section of the fan up to such large distances helps to tightly constrain the pole direction. This is because, while a given projected direction of the pole can be obtained from a large combination of  $\alpha_p$  and  $\delta_p$  values, the curvature and morphology of the fan will be very different because of differences in the cometary latitude of the Earth ( $B$ ) and the Sun ( $B'$ ). The value of  $B$  determines the viewing geometry. The apparent morphology of the fan is very different when the line of sight is inside the fan compared to when it is outside. In the former case, the latitude of source I ( $\phi_1$ ) is smaller than  $B$ . The foreshortening of the fan is asymmetric with respect to the fan axis. For this case,  $\delta_p$  is found to be negative. On the other hand, for positive values of  $\delta_p$ ,  $B$  is smaller than  $\phi_1$ , the line of sight is outside the cone, and the simulations indicate the fan to be very straight. The length, curvature, and cross section of the simulated fans better match the observed fans during 1996 December and 1997 April when the line of sight is within the fan. Furthermore, the fan curvature away from the nucleus is determined by the direction of solar radiation pressure force or  $B'$  on the grains. Hence, the method of determining the pole from the position angle  $P$  can be used as a first guess, while a unique solution is better achieved by carrying out a realistic modeling. Noise has been added to the simulated images to better match the observations.

The fitting was carried out by superposing the simulations on the images. Following Sekanina (2003), we have introduced broad areas for source I and source II. This was done by using clusters of more or less equally spaced point sources to represent a broad source. The pole coordinates  $(\alpha_p, \delta_p)$ , the latitude, and the span in latitude of the sources were adjusted to match the orientation and width of the fans. The latitude range of the sources and approximate relative contributions within

the source that explained the observed features are given in Table 2. The longitude of the sources is indeterminate, as no shell features are seen. The fitted pole positions are given in Table 2. The uncertainty of  $\pm 5^\circ$  in the derived pole position includes the uncertainty in fitting individual images and the spread in the fits to the four images. The uncertainty in the latitude of the sources arises from the uncertainty in the pole solutions through the visual fit. The cometary latitude of the Earth ( $B$ ) and the Sun ( $B'$ ) and the position angle of the projected north pole of the nucleus ( $P$ ) for the fitted pole direction are given in Table 1.

The simulated images on the four dates of observation (Table 1) are shown in the right panels of Figure 3. The images in the left and middle panels are the observed images after normalization with the synthetic coma (§ 2). For the May 15 image, we used the Gaussian-convolved image to improve the S/N. The simulated images are shown superposed on the observed image in the middle panels of Figure 3. In the normalized images of 1997 April 1 and 2, the southwest feature (Fan II, from source II) seen in Figs. 1, 2, and 3 of Schulz et al. (2003) is absent. This may be a result of differences in the techniques of fitting the ambient coma to enhance the features. However, this feature is seen clearly in the processed image of May 15, when the latitude of the Sun was closer to the cometary equator and source II was more favorably illuminated.

## 7. RESULTS AND DISCUSSIONS

A large number of pole solutions may satisfy the observed position angle of a fan in cometary images on a given date. In the present investigation we model the trajectory of the grains in the fan to simulate the observed morphology of the fan. This technique takes advantage of the entire length of Fan I, spanning  $\sim 10^5$  km in the high-quality large-field imaging data on 1997 April 1 provided by M. J. I. Brown & R. L. Webster (2003, private communication) and 1997 April 2 provided by Schulz et al. (2003). The dust tail along the antisunward direction overlaps Fan I in the 1997 April and May images. Therefore, our fit aimed at modeling the curvature of the northern and central regions of this fan.

The present pole solution adequately explains the observed changes in the morphology of Fan I from 1996 December through 1997 May. During 1996 December, cometary latitudes of both the Sun and the Earth were larger than  $\sim 75^\circ$ . Fan I was highly foreshortened. In the May image, this fan is broader compared to its appearance in the April images. This may be because the southern regions of source I on this date were more favorably illuminated than during April (Table 1). Fan II is discernible only in the 1997 May 15 image. The simulated images in the right panels of Figure 3 predict that the assumed period of 0.5 day is large enough for the shells traced by the fan/jet from source II to be resolved. No such shells are seen in the observed image of May 15. The possible reasons could be (1) poor S/N, (2) the assumed period of 0.5 day is long (e.g., a period of 0.25 day may produce a closer unresolved set of shells), (3) the actual rotation period is much longer at several days so that only the first shell is seen and the older ones are faded out, or (4) the source complex is distributed throughout the longitude belt so that there are always regions that are illuminated and contribute to the fan. The derived pole solution of  $\alpha_p = 297^\circ \pm 5^\circ$  and  $\delta_p = -10^\circ \pm 5^\circ$ , which is close to the values of Sekanina (2003), is robust, as the simulation attempts to replicate the initial position angle, width, and curvature of Fan I at large distances.

The 1996 December and 1997 April 2 data were kindly provided by Schulz et al. (2003). We gratefully acknowledge Michael J. I. Brown and Rachel L. Webster for providing the 40 inch (1 m) data of the comet observed by them on 1997 April 1 at the Siding Spring Observatory. This study was possible thanks to the ephemerides of comet Wild 2

by the Solar System Dynamics Group at JPL, Horizons On-Line Ephemeris System (<http://ssd.jpl.nasa.gov/horizons.html>; telnet 6775), authored by Jon Giorgini. It is a pleasure to thank Z. Sekanina for several informative discussions. We are grateful to the referee for very critical and valuable comments.

## REFERENCES

- Delsemme, A. H. 1982, in *Comets*, ed. L. L. Wilkening (Tucson: Univ. Arizona Press), 85
- Farnham, T. L. 2003, *BAAS*, 35, 971
- Farnham, T. L., & Schleicher, D. G. 2002, *BAAS*, 34, 854
- Fink, U., Hicks, M. P., & Fevig, R. A. 1999, *Icarus*, 141, 331
- Finson, M. L., & Probst, R. F. 1968, *ApJ*, 154, 327
- Gurnette, B. L., & Woolley, R. V. D. R. 1961, in *Explanatory Supplement to the Astronomical Ephemeris and the American Ephemeris and Nautical Almanac* (London: HMSO), 342
- Hanner, M. S., & Hayward, T. L. 2003, *Icarus*, 161, 164
- Meech, K. J., & Newburn, R. L. 1998, *BAAS*, 30, 1094
- Rhode, J. R., & Sinclair, A. 1992, in *Explanatory Supplement to the Astronomical Almanac*, ed. P. K. Seidelmann (Mill Valley: University Science Books), 325
- Schulz, R., Stüwe, J. A., Boehnhardt, H., Gaessler, W., & Tozzi, G. P. 2003, *A&A*, 398, 345
- Sekanina, Z. 1981a, *Annu. Rev. Earth Planet. Sci.*, 9, 113
- . 1981b, *AJ*, 86, 1741
- . 1991, in *Comets in the Post-Halley Era*, ed. R. L. Newburn, Jr., M. Neugebauer, & J. Rahe (Dordrecht: Kluwer), 769
- . 2003, *J. Geophys. Res.*, 108, E10, 8112
- Sekanina, Z., & Larson, S. M. 1984, *AJ*, 89, 1408
- Vasundhara, R. 2002, *A&A*, 382, 342
- Vasundhara, R., & Chakraborty, P. 1999, *Icarus*, 140, 221